THE JOURNAL OF BIOLOGICAL CHEMISTRY VOL. 292, NO. 7, pp. 2773–2784, February 17, 2017

Essential Role for Polycomb Group Protein Pcgf6 in Embryonic Stem Cell Maintenance and a Noncanonical Polycomb Repressive Complex 1 (PRC1) Integrity*[S]

Received for publication, October 19, 2016, and in revised form, December 29, 2016 Published, JBC Papers in Press, January 3, 2017, DOI 10.1074/jbc.M116.763961

Wukui Zhao[‡], Huan Tong[‡], Yikai Huang[‡], Yun Yan[‡], Huajian Teng[‡], Yin Xia[§], Qing Jiang[¶], and Jinzhong Qin[‡1]

From the [‡]MOE Key Laboratory of Model Animal for Disease Study, Model Animal Research Center, Nanjing Biomedical Research Institute, Nanjing University, Nanjing 210061, China, [§]School of Biomedical Sciences, The Chinese University of Hong Kong, Hong Kong, China, and [¶]Department of Sports Medicine and Adult Reconstructive Surgery, Nanjing Drum Tower Hospital Affiliated to Medical School of Nanjing University, Nanjing 210008, China

Edited by Xiao-Fan Wang

The Polycomb group (PcG) proteins have an important role in controlling the expression of key genes implicated in embryonic development, differentiation, and decision of cell fates. Emerging evidence suggests that Polycomb repressive complexes 1 (PRC1) is defined by the six Polycomb group RING finger protein (Pcgf) paralogs, and Pcgf proteins can assemble into noncanonical PRC1 complexes. However, little is known about the precise mechanisms of differently composed noncanonical PRC1 in the maintenance of the pluripotent cell state. Here we disrupt the Pcgf genes in mouse embryonic stem cells by CRISPR-Cas9 and find Pcgf6 null embryonic stem cells display severe defects in self-renewal and differentiation. Furthermore, Pcgf6 regulates genes mostly involved in differentiation and spermatogenesis by assembling a noncanonical PRC1 complex PRC1.6. Notably, Pcgf6 deletion causes a dramatic decrease in PRC1.6 binding to target genes and no loss of H2AK119ub1. Thus, Pcgf6 is essential for recruitment of PRC1.6 to chromatin. Our results reveal a previously uncharacterized, H2AK119ub1-independent chromatin assembly associated with PRC1.6 complex.

The Polycomb group proteins are a conserved family of epigenetic transcriptional repressors with well defined roles in stem cell maintenance and development (1, 2). Polycombs participate in one of two distinct multiprotein complexes known as Polycomb repressive complex 1 (PRC1)[2] and PRC2. In mammals the PRC2 complex is composed of the core components Eed, Ezh2, and Suz12 and catalyzes the trimethylation of lysine 27 on histone H3 (H3K27me3). The canonical PRC1 complex (c-PRC1) contains orthologs of *Drosophila* Polycomb (Cbx2/4/6/7/8), Posterior sex combs (pcgf1–6), Sex comb extra (Ring1A/B), and Polyhomeotic (Phc1–3) (3). The c-PRC1 complex can recognize and bind to H3K27me3 through Cbx proteins and thus facilitate the recruitment of c-PRC1 to PRC2-target genes. The heterodimeric E3 ligase Ring1B/Pcgf1–6 in the c-PRC1 complex then catalyzes the monoubiquitination of histone H2A at lysine 119 (H2AK119ub1), which is thought to contribute to chromatin compaction and gene silencing (1, 2, 4). However, this hierarchical model of sequential PRC2-dependent PRC1 recruitment has been challenged recently by the biochemical characterization of noncanonical PRC1 complexes, which do not require PRC2 activity to mediate H2AK119ub1 (5–7). On the biochemical level, the noncanonical PRC1 complexes contain Rybp/Yaf2 but no CBX or Phc subunits. Recently, proteomic profiling of PRC1 components has revealed the existence of six distinct groups as PRC1.1-PRC1.6 based on available Pcgf subunit, yet their diverse biological and molecular activities remain to be fully understood (8).

Recently, we demonstrated that mice deficient in *L3mbtl2* gene, encoding a genuine component of PRC1.6 complex in ES cells, displayed embryonic lethality soon after implantation (9). Accordingly, ES cells lacking L3mbtl2 showed a severe proliferation defect and were unable to properly differentiate. *L3mbtl2* null ES cells exhibited aberrant de-repression of lineage-specific genes, especially germ cell-related gene. Notably, genome wide studies revealed that most L3mbtl2 target genes were not bound by canonical PRC1 and PRC2. Consistent with this finding, we detected H2AK119ub1 at 10-fold lower levels than that at canonical PRC1 targets, and the absence of L3mblt2 at promoters did not correlate with the change of H2AK119ub1 enrichment, indicating H2AK119ub1 is not involved in L3mbtl2-mediated gene repression. We also noted that L3mbtl2 is required for optimal recruitment of some components (*i.e.* Ring1B, E2F6, G9A, and Hdac1) of PRC1.6 complex to selected germ cell genes (9). These observations prompted us to further explore the precise functions of each subunit in PRC1.6 and delineate the relative contributions of each to maintain a balanced state of gene expression in ES cells.

* This work was supported by grants from the National Natural Science Foundation of China (31471387 and 31671532) and by the 2015 Shuangchuang Program of Jiangsu Province (to J. Q.) The authors declare that they have no conflicts of interest with the contents of this article.

[S] This article contains supplemental Tables 1–3 and Figs. 1–4.

Microarray data were deposited at the Gene Expression Omnibus under accession number GSE92476.

[1] To whom correspondence should be addressed: MOE Key Laboratory of Model Animal for Disease Study, Model Animal Research Center, Nanjing University, 12 Xuefu Rd., Nanjing, Jiangsu 210061, China. Tel.: 86-025-58641504; Fax: 86-025-58641500; E-mail: qinjz@nicemice.cn.

[2] The abbreviations used are: PRC1 and 2, Polycomb repressive complex 1 and 2, respectively; ES, embryonic stem; MEF, mouse embryonic fibroblast; sgRNA, single guide RNA; EB, embryoid body; LIF, leukemia inhibitory factor; qPCR, quantitative PCR; MBT, malignant brain tumor.

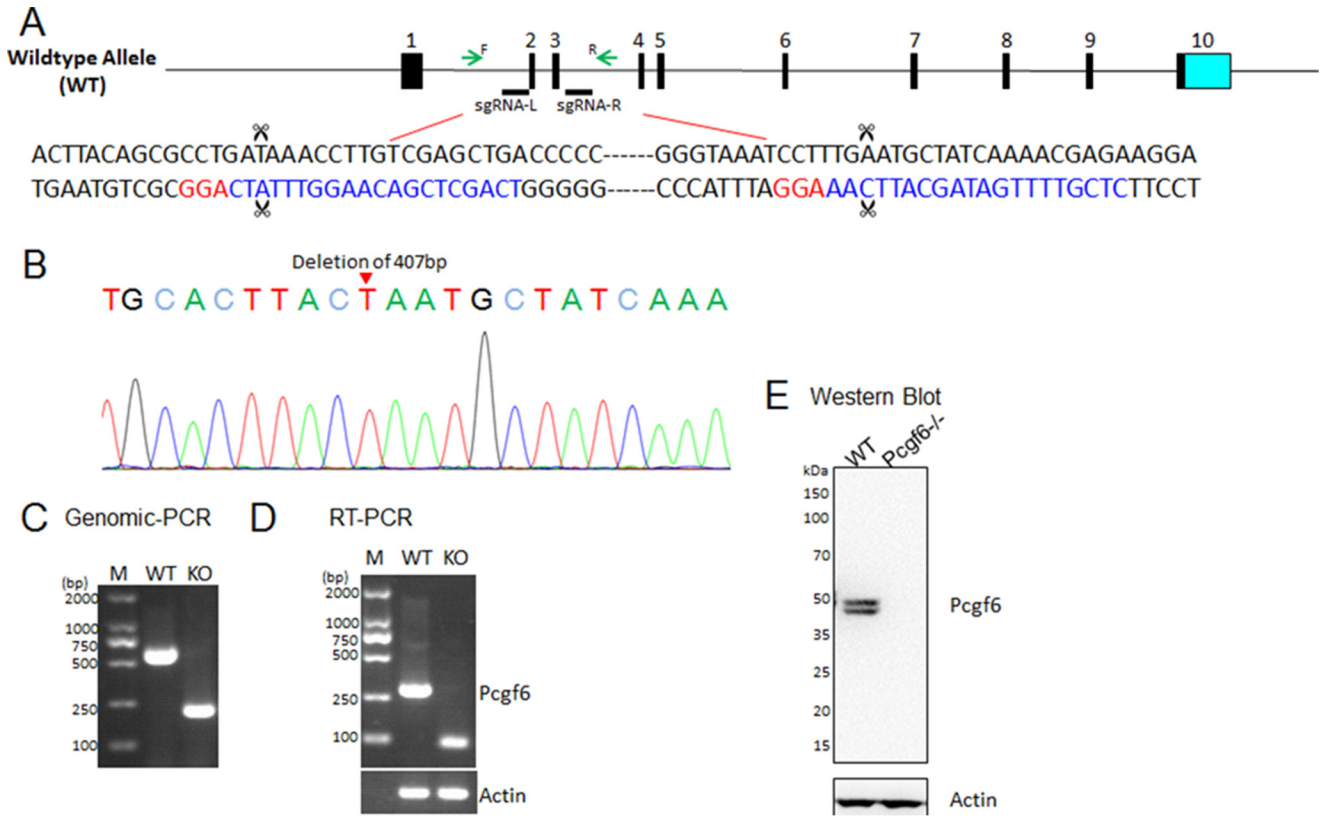

FIGURE 1. **Generation of Pcgf6 null ES cells by two sgRNAs (spanning exon 2 to 3) guiding Cas9.** *A*, schematic overview of the strategy to delete a genomic fragment (407 bp) containing exons 2–3 of the pcgf6 gene. PAM sequences are in *red* after the sgRNA sequence highlighted in *blue*. The *scissor symbol* indicates the predicted Cas9 cleavage position of the sgRNA sequence. The locations of genomic PCR primers (*F*, forward; *R*, reverse) are indicated by *green arrows* (external to the deletion). *B*, direct sequencing of the PCR product from pcgf6$^{-/-}$ confirmed deletion of the 407-bp DNA fragment. Each DSB occurred exactly 3 bp upstream of the PAM sequence. *C*, genotyping of pcgf6 knock-out ES cells using primers upstream and downstream of the deleted region. *D*, RT-PCR analysis for residual *Pcgf6 mRNA* revealed a shorter band in the mutant consistent with a shorter message as predicted. *β*-Actin served as a loading control. *E*, Western blot analysis using an antibody recognizing pcgf6 demonstrated the absence of the protein in knock-out ES cells. Note that no mutant protein band was detected from pcgf6$^{-/-}$ ES samples.

Pcgf6 (also known as MBLR) has been characterized as a subunit of the repressive E2F6-containing complex in HeLa cells together with E2F6, DP1, HP1γ, Max, Mga, L3mbtl2, Ring1B, Ring1A, G9a, GLP, and Yaf2 (10). Subsequently, the majority of these previously described components were identified to be associated with L3mbtl2 in ES cells (9), and this complex was categorized into a noncanonical PRC1 subgroup referred to as PRC1.6 in somatic cells (8). Reportedly, Pcgf6 was previously identified in an RNAi screen for the factors involved in maintenance of ES cell pluripotency (11). In recent knockdown studies, Pcgf6 was identified as a key regulator of ES cell pluripotency and iPS reprogramming (12, 13). Due to residual Pcgf6 activity caused by incomplete and transient knockdown, we hypothesized that Pcgf6 knock-out may elicit more profound effects.

Here, we initially examined the role of Pcgf family in ES cells via the CRISPR/Cas9 system, and Pcgf6 was identified as a strong candidate vital for ES cell self-renewal. In addition to the severe proliferation defect, Pcgf6 null ES cells showed unscheduled expression of genes mostly involved in differentiation and spermatogenesis and skewed differentiation into the endoderm lineage in embryoid bodies *in vitro*. Pcgf6 was necessary for the stability of the PRC1.6 complex, as ES cells deleted in Pcgf6 did not have a L3mbtl2-Max and Ring1B-Rybp association. Interestingly, although we detected high levels of PRC1.6 complex on Pcgf6 target promoters, its enrichments correlated with almost baseline levels of H2AK119ub1. Furthermore, despite the loss of Pcgf6 resulting in dramatically reduction of this complex at these promoters, no significant changes in the status of H2AK119ub1 were observed. This finding implies that PRC1.6 complex functions independently of the enzymatic activity of Ring1B. Taken together, our data strongly indicate that Pcgf6 is important for the stable assembly and efficient recruitment of the PRC1.6 complex to maintain ES cell state.

Results

Targeted Deletion of Pcgf Family Genes by CRISPR-Cas9 with a Pair of sgRNAs—Polycomb Group RING finger homologs (Pcgf1–6) are extensively considered to be integral subunits of PRC1 in ES cells yet no systematic investigation of their role in ES cell property has been reported to date (8). We thus generated individual Pcgf-deficient ES cell line by utilizing CRISPR-Cas9 technology (14, 15). For each Pcgf member, we first designed a pair of single guide RNAs (sgRNAs) for two sites flanking DNA fragment containing one or two exons encoding the RING domain of Pcgf (Fig. 1*A* and supplemental Figs. 3*A* and 4*A*). Genomic DNA was isolated from the mouse ES cell colonies transfected with plasmids encoding Cas9 and a pair of sgRNAs (14). Subsequently, deletions were determined by PCR with primers outside the expected cleavage site (Fig. 1*C* and supplemental Figs.

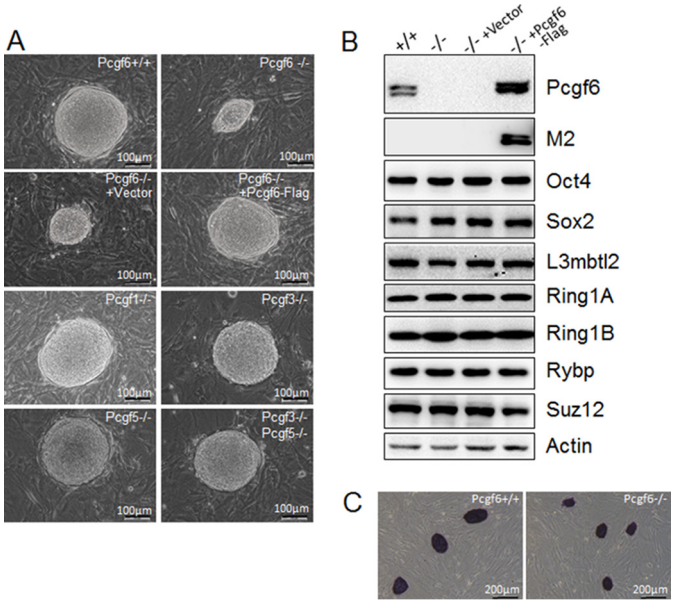

FIGURE 2. **Pcgf6 is an indispensable Pcgf family member in ES cell self-renewal.** *A*, phase-contrast pictures of ES cells of indicated genotypes growing on feeders cells. Notably, *Pcgf6*$^{-/-}$ ES cell colony size was strikingly reduced but fully restored by lentiviral expression of Pccgf6-F. Shown was colony-size 6 days after seeding single cell suspensions onto MEF feeder layers in the presence of LIF. *B*, Western blot demonstrating changes in the levels of Oct4, Sox2, and PcG proteins and transcription factors in ES cells of the indicated genotypes. β-Actin was used as a loading control. *C*, the maintenance of alkaline phosphatase positive colonies in *Pcgf6*$^{-/-}$ ES cells.

3*C* and 4*C*). Additionally, the precision of targeted deletion was confirmed by Sanger sequencing of the PCR products (Fig. 1*B* and supplemental Figs. 3*A* and 4*A*). Targeted deletions were further verified by reverse transcription (RT)-PCR and sequencing (Fig. 1*D* and supplemental Figs. 1, 3*B*, 3*D*, 4*B*, and 4*D*). Finally, Western blot analysis showed a complete loss of Pcgf protein in targeted deletion mutant ES cells (Fig. 1*E* and supplemental Figs. 3*E* and 4*E*).

Pcgf6 Is the Only Pcgf Family Member Essential for ES Cell Self-renewal—To characterize ES cells deficient in a Pcgf member, we analyzed their ability to form colonies after seeding on mitomycin-C-irradiated mouse embryonic fibroblasts (MEFs). ES cells were dissociated with trypsin and replated to allow the ES cells to expand into colonies. The Pcgf null ES cells were viable and retained a typical undifferentiated ES cell morphology when cultured on feeder layers, forming tight dome-shaped colonies indistinguishable from those formed by wild type cells (Fig. 2*A*). In addition, the lack of deficits in ES cell proliferation in *Pcgf3* or its closest family member *Pcgf5* single knock-out is not likely caused by each other's compensation because double knock-out ES cells (*Pcgf3*$^{-/-}$ *Pcgf5*$^{-/-}$) did not exhibit significantly worse defects than single knock-out. However, upon loss of *Pcgf6* but not *Pcgf1*, *Pcgf3*, and *Pcgf5*, ES cell colony size was drastically reduced (in which the doubling time increased from ~13 h to ~22 h). Remarkably, however, lentiviral expression of FLAG-tagged Pcgf6 entirely restored normal ES cell growth and protein expression (Fig. 2*A*). To test whether Pcgf6 might be involved in the proliferation of other cell types, mouse primary embryonic fibroblasts were transfected with a pair of sgRNAs targeting Pcgf6 as described for ES cells. In contrast to ES cells, MEFs retained normal proliferation after Pcgf6 deletion (supplemental Fig. 2). These findings corroborate previous observations made by us (9) and imply that Pcgf6 selectively regulates proliferation in the context of ES cells. Consistent with their undifferentiated morphology, Pcgf6$^{-/-}$ ES cells maintained similar levels of pluripotency markers (Oct4, Nanog, and Sox2) and alkaline phosphatase activity to wild type cells (Fig. 2, *B* and *C*). Additionally, Pcgf6$^{-/-}$ ES cells retained near wild type protein levels of other components of PRC1.6 (L3mbtl2, Ring1A, Ring1B, Rybp) as well as PRC2 member Suz12 (Fig. 2*B*). Given that Pcgf4/Bmi1 knock-out mice are viable and mice lacking Pcgf2/mel-18 survive to birth (16), we hypothesize that Pcgf6 is the only member of the Pcgf family that is critical for the maintenance of the self-renewal state of ES cells. Therefore, in the rest of this paper we will specifically focus on understanding the functional and mechanistic role of Pcgf6 in regulation of pluripotency.

ES Cells Deficient in Pcgf6 Displays Skewed Differentiation toward Endoderm—To examine whether Pcgf6 deletion leads to a specific defect in differentiation, Pcgf6$^{-/-}$ and control ES cells were tested for their capacity to form embryoid bodies (EBs) *in vitro*. Upon leukemia inhibitory factor (LIF) withdrawal, ES cells form cell aggregates known as EBs (Fig. 3*A*) in which cells differentiate into the three germ layers (endoderm, mesoderm, and ectoderm) (17). This process is highly correlated with expression of a panel of specific lineage markers. *Pcgf6*$^{-/-}$ ES cells did form EBs, but they were greatly reduced in size than those of the wild type during the differentiation process (Fig. 3, *B* and *C*). The RT-quantitative PCR (qPCR) analysis revealed that Pcgf6$^{-/-}$ EBs expressed markers for definitive ectoderm, mesoderm, and endoderm, whereas the expression levels of the pluripotency markers Oct4 and Nanog were subsequently down-regulated during differentiation in EBs deficient in Pcgf6 as they were in control cells (Fig. 3*D*). However, throughout *Pcgf6*$^{-/-}$ EB culture the expression of endoderm markers including Sox17, Gata6, Gata4, and Foxa2 was dramatically increased with respect to control EBs, indicating that Pcgf6 prevents the differentiation of ES cells into endoderm (Fig. 3*D*). Remarkably, lentiviral expression of FLAG-tagged Pcgf6 was able to rescue the pattern of expression of endoderm markers to levels similar to those in control cells. Notably, we previously reported that L3mbtl2 represses the expression of Sox17 and Foxa2 (9), key regulators essential for all endodermal lineage development, via direct binding to their promoter regions. Moreover, the data in this manuscript demonstrated that Pcgf6 is required for the ordered chromatin recruitment of L3mbtl2 (see Fig. 8*A*). Therefore, we propose that Pcgf6 displays specificity toward endoderm formation through modulating L3mbtl2 activity.

Pcgf6 Null ES Cells Show Unscheduled Expression of Genes Mostly Involved in Differentiation and Spermatogenesis—To understand the mechanistic basis of the requirement for Pcgf6 in ES cell maintenance, we analyzed the impact of loss of Pcgf6 function on mRNA expression. For this, we established genome-wide gene expression profiles of wild type, *Pcgf6*$^{-/-}$, and *Pcgf6*$^{-/-}$ rescued with Pcgf6-F ES cells using Agilent microarrays. Microarray analysis identified 2542 genes with >2-fold altered expression levels in Pcgf6$^{-/-}$ compared with wild type ES cells (Fig. 4*A*, supplemental Table 3). Strikingly,

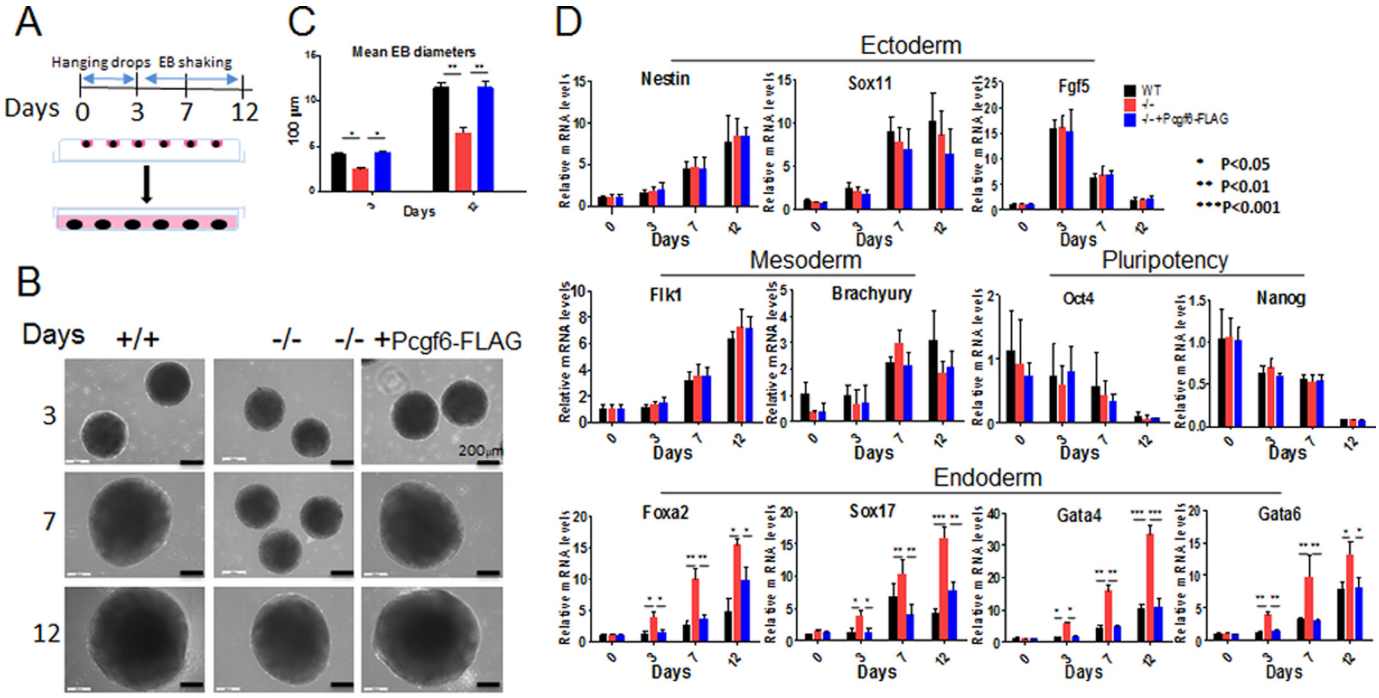

FIGURE 3. **EB formation and differentiation.** *A*, EBs were formed in hanging drops and subsequently maintained in rotating cultures. *B*, ES cells lacking Pcgf6 retained the potential to form EBs after LIF withdrawal, but EBs were compromised for growth. *C*, *bar graphs* indicate the mean diameters of 20 EBs from cultures of indicated genotypes. *D*, real-time RT-PCR was used to measure the expression of pluripotency and lineage-specific markers in control and *Pcgf6*$^{-/-}$ mRNA samples derived from ES cells and in 12-day differentiated EBs. Marker genes for all germ layers were expressed in mutant and wild type EBs, but endodermal marker genes were significantly overexpressed at different time points in Pcgf6$^{-/-}$ EBs. Shown is the mean relative mRNA expression (ratio of measured mRNA/to β-actin mRNA).

re-expression of Pcgf6-F was accompanied by 57% of these genes changed >2-fold in the opposite direction (Pcgf6-F-infected cells compared with Pcgf6$^{-/-}$). Together, these criteria revealed a set of 1444 Pcgf6 target genes. 1179 (82%) genes were up-regulated in the absence of Pcgf6, whereas only 265 genes (18%) were down-regulated (Fig. 4*B*). Expression of some of the transcripts identified as up-regulated by microarray analysis was evaluated independently by RT-qPCR (see Fig. 7*A*). Therefore, Pcgf6 acts predominantly as a transcriptional repressor in ES cells. Gene Ontology (GO) analysis for these up-regulated genes found significant enrichment with several categories consistent with the phenotype we observed as well as with germ-cell-related gene ontology terms (*i.e.* meiosis, spermatogenesis) (Fig. 4*C*). Furthermore, of the 49 up-regulated genes with a >10-fold increase in expression, 20 either have been reported to be essential in spermatogenesis or were expected to have a function in meiosis or spermatogenesis based on unique expression profile or molecular property (Fig. 4*D*) (9, 18). Of note, the ES cells we used for our experiments were male (XY). Our ongoing study is to define the role of Pcgf6 in spermatogenesis-related events in a XX-ES cell line. Moreover, although only 9% of genes up-regulated >2-fold in L3mbtl2$^{-/-}$ ES cells overlapped with these in Pcgf6$^{-/-}$ cells through microarray analysis (see Fig. 8*D*), the top up-regulated genes were similar between Pcgf6 and L3mbtl2 knock-out cells (*i.e.* these six genes mentioned below) by RT-qPCR (see Figs. 7*A* and 8*B*). This discrepancy may be due to the sensitivity limits of a hybridization-based microarray approach. Taken together, these results indicate that Pcgf6 controls a transcriptional cascade to govern ES cell self-renewal, pluripotency, and repression of germ cell-specific genes in ES cells.

Identification of the Pcgf6 Region Essential for Its Biological Activities in ES Cells—To search for structural features of Pcgf6, we took advantage of the above-mentioned observation that reexpression of FLAG-tagged Pcgf6 fully restored normal ES cell growth and protein expression. We generated serial deletion and point mutants and tested their ability to rescue self-renewal and transcriptional activity defects associated with deletion of the *Pcgf6* gene (Fig. 5*A*). As summarized in Fig. 5*A*, N-terminal deletion mutants (Δ2–50, Δ51–100, and Δ2–100) fully restored wild type levels of growth in ES cells. However, further progressive deletion mutants from the N-terminal 100 amino acids virtually eliminated their ability to rescue the colony-growth defect. Notably, deletions of the RING domain (Δ137–175) and even point mutations (C137A/C140A, C153A/H155A) of the zinc-coordinating residues abolished Pcgf6's potential to rescue proliferation. It has previously been documented that Ser^{34} of Pcgf6 is phosphorylated during mitosis (19). We found that Pcgf6 antibody detected two differently migrating bands in ES cells (Fig. 1*E* and 2*B*). To confirm that Ser^{34} of Pcgf6 was phosphorylated, it was replaced with alanine by site-directed mutagenesis (S34A). We found that the substitution of Ser^{34} abolished the slowly migrating band of Pcgf6 when S34A was stably expressed in ES cells (Fig. 5*B*). Accordingly, N-terminal deletion mutants (Δ2–50 and Δ2–100), but not other deletion mutants, were accompanied by the disappearance of the slowly migrating band, confirming that Ser^{34} is the only phosphorylation site in Pcgf6. Nonetheless, as shown

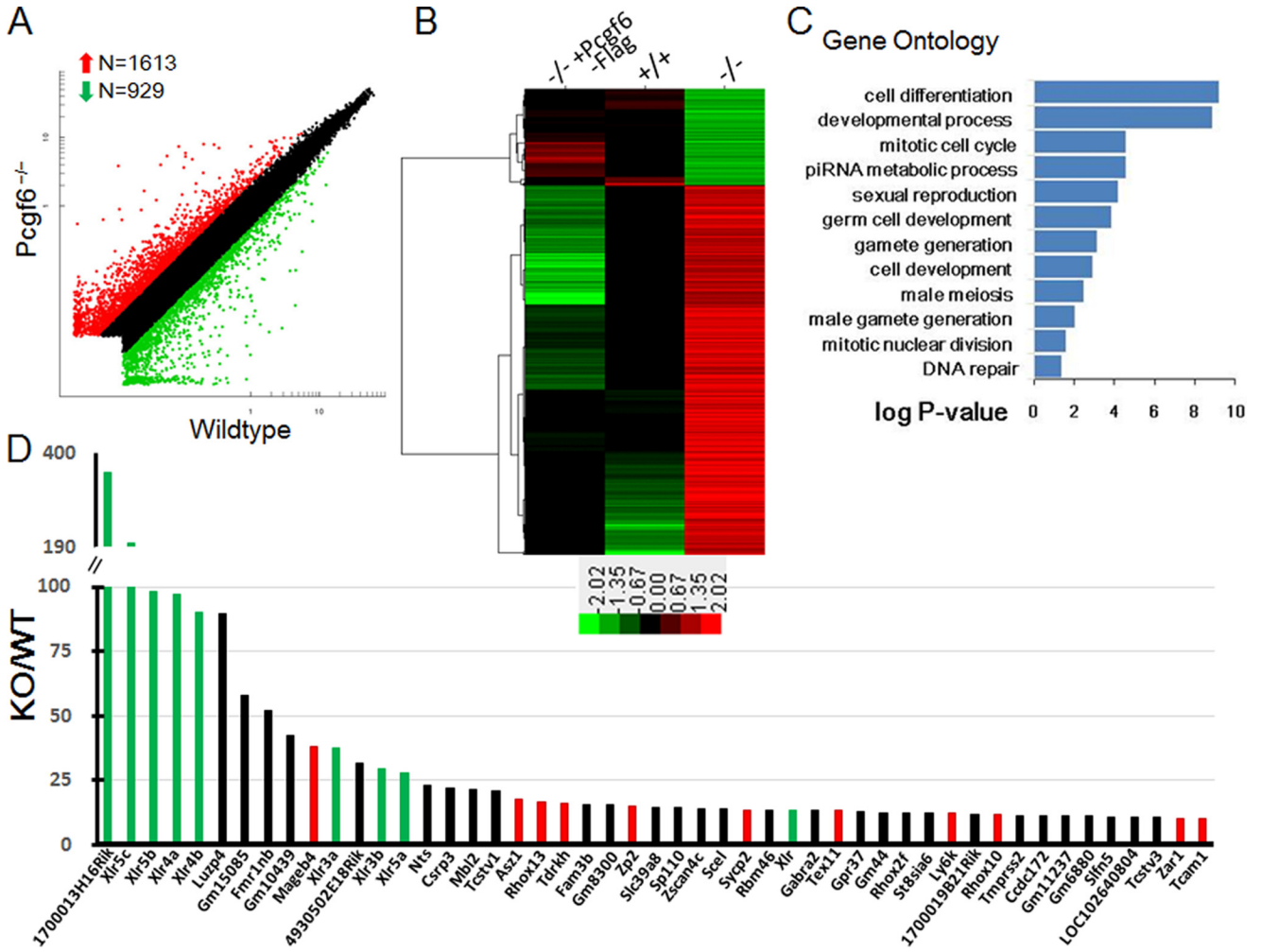

FIGURE 4. **Gene expression profiling in ES cells lacking *Pcgf6*.** *A*, $\log_2$ expression values in Pcgf6$^{-/-}$ *versus* wild type ES cells from expression microarray. Probes were considered to be up-regulated (*red*) or down-regulated (*green*) if they had a $\log_2$-fold change of >1 or <-1, respectively. The number of differentially expressed genes they represented is indicated. *B*, microarray heat map depicting gene expression in wild type, *Pcgf6*$^{-/-}$ and Pcgf6$^{-/-}$ infected with Pcgf6-F ES cells. *Columns* showed 2542 *bars* that represent genes with >2-fold expression differences between wild type (*second column*) and *Pcgf6*$^{-/-}$ ES cells (*third column*). *C*, Gene Ontology analysis of Pcgf6 target genes. Shown is Gene Ontology analysis of biological functions of Pcgf6 up-regulated target genes; *p* values were plotted in −log; *PiRNA*, Piwi-interacting RNA. *D*, -fold changes in the expression of the top 49 genes, each of which showed >10-fold up-regulation in Pcgf6$^{-/-}$ compared with wild type. *Red bars*, germ cell-specific genes; *green bars*, XLR (X-chromosome-linked lymphocyte-regulated) gene family. Microarray data were deposited at the Gene Expression Omnibus under accession number GSE92476.

in Fig. 5, *A* and *C*, like Δ2–50, Δ51–100, and Δ2–100, S34A fully restored wild type levels of ES cell growth and the expression of Pcgf6 target genes.

We next compared the contribution of those mutants to transcriptional regulation. As expected, wild type expression levels of Pcgf6 target genes (ZSCAN4C, TDRKH, and RHOX10) were restored in the Pcgf6 N-terminal deletion mutants (Δ2–50, Δ51–100, and Δ2–100) reconstituted null cells (Fig. 5*C*). All deletions downstream from residue 100 abrogate transcription ability. Thus, the N-terminal 100 amino acid residues are dispensable for Pcgf6-mediated ES cell self-renewal and transcriptional repression of target genes. When considered as a whole, the data from colony and transcription assays clearly indicate that a region extending from residue 100 to the C terminus, although required for self-renewal, suppresses Pcgf6-mediated transcription. Within this the RING domain, Δ137–175 therefore appears to be critical to the proper function of Pcgf6 in ES cells.

Pcgf6 Is Required for PCR1.6 Complex Integrity—To demonstrate an *in vivo* interaction between Pcgf6 and other components in PRC1.6 complex, we performed co-immunoprecipitations in protein extracts of wild type and Pcgf6$^{-/-}$ ES cells using a Pcgf6-specific antibody (IgG as a control). Endogenous Pcgf6 readily co-immunoprecipitated with endogenous L3mbtl2, Max, Ring1B, and Rybp, but not Pcgf3 or Pcgf5, in wild type ES cells, whereas Pcgf6 antibody failed to precipitate these components in the complex from Pcgf6$^{-/-}$ extracts (Fig. 6*A*). The interaction of Pcgf6 with L3mbtl2, Ring1B, and Rybp was further confirmed by reverse endogenous co-immunoprecipitation with antibodies specific for L3mbtl2, Ring1B, and Rybp, three of which coprecipitated Pcgf6, whereas preimmune IgG did not. In striking contrast, we found that L3mbtl2 and Max were not detected in the anti-Ring1B or anti-Rybp immunoprecipitated samples and that Ring1B and Rybp were not detected in the samples immunoprecipitated with anti-L3mbtl2 antibodies in Pcgf6$^{-/-}$ ES cells, although they existed

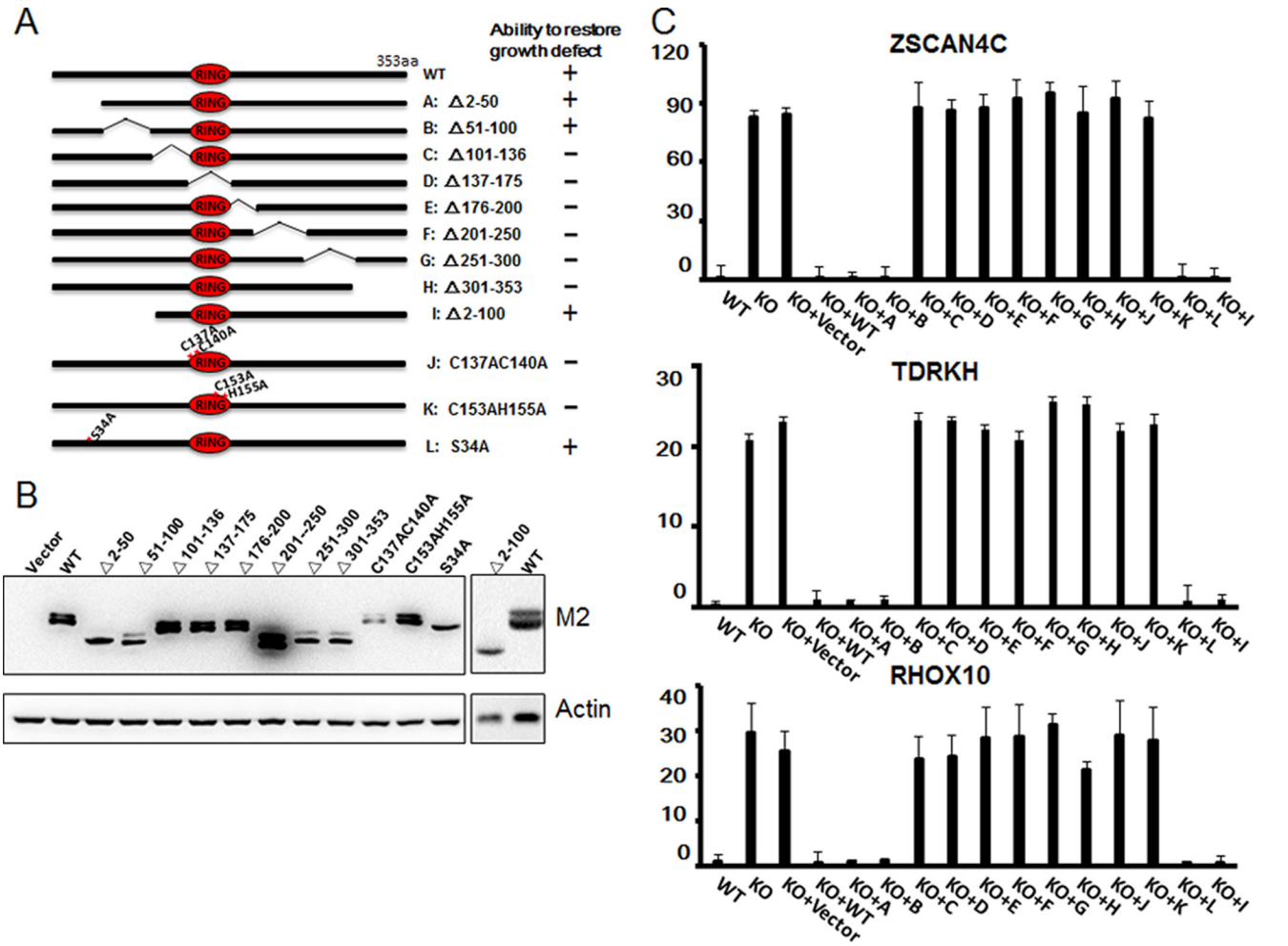

FIGURE 5. **Structure/function analysis of Pcgf6 in ES cells.** *A*, schematic representation of PCGF6 deletion and point mutants in this study and summary of their ability to rescue Pcgf6$^{-/-}$ ES cell growth defect. The *thick solid bars* indicate the region of Pcgf6 encoded by each mutant. Deletions in the Pcgf6 coding regions are depicted as *thin bent lines*. The *numbers* representing each mutant also indicate the amino acid residue numbers at the boundaries of the deletions. *B*, Western blot analysis demonstrated the protein expression level of all mutants. Serial Pcgf6 deletion constructs were transfected into Pcgf6$^{-/-}$ ES cells and analyzed by Western blotting with anti-FLAG antibody. Of note, a Ser^{34}→Ala^{34} (S34A) point mutant and deletion mutants (Δ2–50, Δ2–100) of Pcgf6 were not phosphorylated. *C*, transcriptional ability of Pcgf6 deletion and point mutants. Changes in expression levels for the selected Pcgf6 target genes as determined by real-time PCR. Expression levels were normalized to a β-actin control and depicted as -fold changes relative to the wild type ES cells. *Error bars* are based on the S.D. as derived from triplicate PCR reactions.

in the same complex in wild type extracts. Unexpectedly, the interaction between L3mbtl2 and Max was severely impaired in Pcgf6$^{-/-}$ ES cells, whereas depletion of Pcgf6 did not disrupt the interaction between endogenous Rybp and Ring1B (Fig. 6*A*), indicating that Pcgf6 is required for interaction between L3mbtl2-Max and Ring1B-Rybp. Thus, the integrity of the PRC1.6 complex depends on the presence of Pcgf6.

To provide an *in vivo* test of the Pcgf6 interaction domain, some of the above-mentioned FLAG-tagged deletion and point mutants were stably expressed in Pcgf6$^{-/-}$ ES cells. Cell lysates were prepared, and the FLAG-tagged proteins were immunoprecipitated with anti-FLAG antibodies followed by Western blotting with the antibodies indicated in Fig. 6*B*. L3mbtl2, Ring1A, Ring1B, and Rybp binding were observed in the FLAG immunoprecipitates from cells reconstituted with the full-length wild type or point mutant S34A (Fig. 6*B*). The RING domain deletion (Δ137–175) and point mutations (C137A/C140A), however, failed to coimmunoprecipitated Ring1A, Ring1B, and Rybp although it retained the ability to coprecipitate with L3mbtl2 to an extent similar to that of the full-length wild type (Fig. 6*B*). These indicate that the RING domain is essential to accommodate interaction of Pcgf6 with Ring1A, Ring1B, and Rybp, whereas the L3mbtl2-binding site is mapped to the C-terminal domain of Pcgf6. Together, our data suggest that Pcgf6 bridges Ring1B and Rybp with chromatin protein L3mbtl2, which in turn brings together the PRC1.6 to the promoters of target genes.

The Pcgf6-L3mbtl2 Interaction Is Required for the Proper Targeting of PRC1.6 Complex to Target Genes—As mentioned previously, loss of *Pcgf6* in ES cells was not associated with overall expression changes of its interactor Ring1B. Consistent with this, the chromatin modification deposited by this enzyme (H2AK119ub1) was not globally changed (Fig. 7*D*). On the contrary, in the absence of Ring1B (Ring1B$^{-/-}$), levels of H2AK119ub decreased markedly. It is worthy of note that residual levels of H2AK119ub are most likely due to the expression of Ring1A, the closely related homolog of Ring1B in ES cells (20).

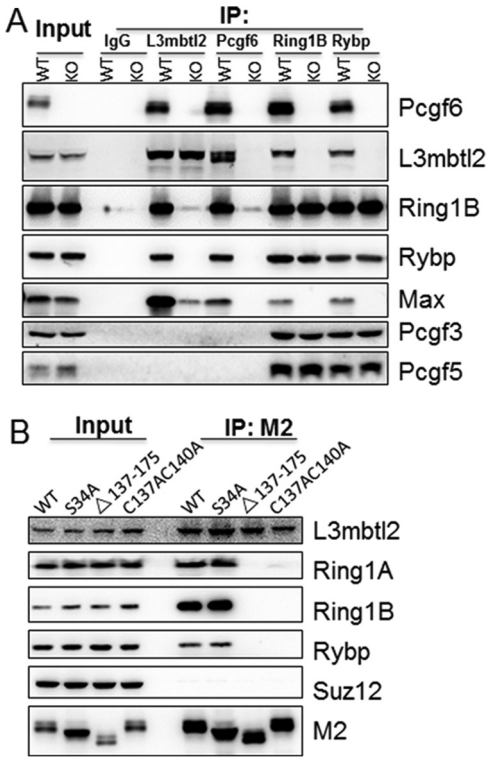

FIGURE 6. **Essential role for Pcgf6 in PRC1. 6 complex integrity.** *A*, physical interaction of L3mbtl2, Pcgf6, Ring1b, and Rybp in cell extracts from wild type and *Pcgf6*$^{-/-}$ ES cells demonstrated by reciprocal co-immunoprecipitation assays. Antibodies used for immunoprecipitation (*IP*, *top*) and immunoblotting are indicated. *B*, the Ring domain is required for interaction of Pcgf6 with Ring1a, Ring1b, and Rybp. FLAG-Pcgf6 wild type (*WT*) and mutants (*S34A*, *Δ137–175*, *C137A/C140A*) stable-transfected into *Pcgf6*$^{-/-}$ ES cells were immunoprecipitated with the FLAG antibody and analyzed by Western blot with the indicated specific antibodies.

To determine whether Pcgf6 is required for PcG chromatin binding by using *Pcgf6*$^{-/-}$ ES cells, we probed six Pcgf6 direct target genes (TDRKH, TCAM1, LUZP4, RHOX10, MAGEB4, and ZSCAN4C) and three cPRC1 targets (Sox17, Foxa2, and Hoxb8). Their differential expression and Pcgf6 occupancy status were confirmed by RT-qPCR and chromatin immunoprecipitation (ChIP)-qPCR, respectively (Fig. 7, *A*, B, and C). We first studied the effect of ablating Pcgf6 on the recruitment of c-PRC1 and PRC2 to their targets. As expected, Rybp and Ring1B , shared components between variant PRC1 and cPRC1 in ES cells, and Suz12 (a core component of PRC2) were strongly enriched at PRC1/2 targets (Fig. 8*A*). Accordingly, high levels of H3K27me3 and H2AK119ub1 were detected at Sox17, Foxa2, and Hoxb8, and moreover, their enrichments were not altered after disruption of Pcgf6 (Fig. 7*C*). As expected, Pcgf6 and L3mbtl2 were absent at these targets and were not altered after knock-out of Pcgf6. Thus, Pcgf6 is not required for the recruitment or activity of PRC1 or PRC2 at c-PRC1/2-bound targets.

Next, we wanted to test whether loss of Pcgf6 protein in PRC1.6 complex affects the chromatin targeting of other members of the complex *in vivo*. ChIP-qPCR experiments demonstrated that Pcgf6 colocalized with other components in the PRC1.6 complex (*i.e.* Ring1B, L3mbtl2, and Rybp) on Pcgf6 target promoters (Fig. 8*A*). However, their enrichments were dramatically reduced in the Pcgf6$^{-/-}$ ES cells at these target genes. Of note, despite our observation that global H3K27me3 was not affected by loss of Pcgf6, we observed that H3K27me3 enrichment was reduced by 2–3-fold in the Pcgf6$^{-/-}$ ES cells at these specific targets of Pcgf6 (Fig. 7*C*). As these targets did not bind PRC2 (*i.e.* Suz12), the H3K27me3 signal may be generated by a component of PRC1.6, G9a, which has been shown to methylate H3K27 *in vivo* (21). Unexpectedly, despite exhibiting high levels of Ring1B, the promoters of these targets were associated with extremely low amounts of H2AK119ub1, whereas the loss of Pcgf6 at these promoters did not correlate with the change of H2AK119ub1 enrichment, suggesting that transcriptional repression by Pcgf6 (or even PRC1.6 complex) is likely independent of the H2AK119ub1 mark (Fig. 7*C*). Intriguingly, the targeting defect due to the loss Pcgf6 is reminiscent of the phenotype we previously observed in ES cells after deletion of L3mbtl2 (9). In L3mbtl2$^{-/-}$ ES cells, there was a greatly reduced occupancy of the PRC1.6 components (*i.e.* Ring1B, E2F6, G9A, and Hdac1) compared with wild type ES cells. Additionally, ChIP-qPCR was done on the L3mbtl2$^{-/-}$ cells to determine the effect of L3mbtl2 depletion on Pcgf6 occupancy at specific target promoters (Fig. 8, *B* and *C*). We found that Pcgf6 was mostly displaced from its targets in L3mbtl2 null ES cells. Although it has been shown that L3mbtl2 is able to bind to chromatin through its malignant brain tumor (MBT) domains *in vitro* (22), our data clearly indicated L3mbtl2 alone is not enough for the recruitment of the whole PRC1.6 complex, a result consistent with our previous finding that Ring1B was not entirely lost at L3mbtl2's targets after L3mbtl2 disruption. Together, our observations suggest that Pcgf6 cooperatively interacts with chromatin-associated protein L3mbtl2 and that mutual interaction plays a significant role in coordinating the assembly and chromatin targeting of the PRC1.6 complex.

Discussion

As mentioned earlier, several different noncanonical-PRC1 complexes have been identified recently, all of which are composed of the Ring1B together with different combinations of the other various subunits (and or family members) with distinct genomic localization and lineage expression patterns (8, 23, 24). Given their recent discovery, the potentially biological functions of each type of noncanonical PRC1 complex remain largely unknown. Using CRISPR-Cas9 technology, we have generated single and double mutants homozygous for the *Pcgf* family in ES cells. Although these mutants retain ES cell morphology, alkaline phosphatase activity, and express high levels of Oct4 and Sox2, Pcgf6-deficent ES cells display significant growth retardation compared with control (Fig. 2, *A* and *B*). Additionally, Pcgf6-deleted ES cells fail to efficiently differentiate along endodermal lineages during embryoid body formation (Fig. 3). These results are similar to those observed for L3mbtl2$^{-/-}$ ES cells (9), underscoring the molecular and functional overlap between Pcgf6 and L3mbtl2 in ES cells. Several recent reports propose that, similar to PRC2 (25, 26), PRC1 is required for ES cell differentiation but not for ES cell self-renewal (3, 4, 27). However, this conclusion was drawn based on the studying of c-PRC1. Our present study together with the previous investigations by us and others clearly illustrate the critical roles of Pcgf6, L3mbtl2, Max, and Mga (9, 11, 28–30),

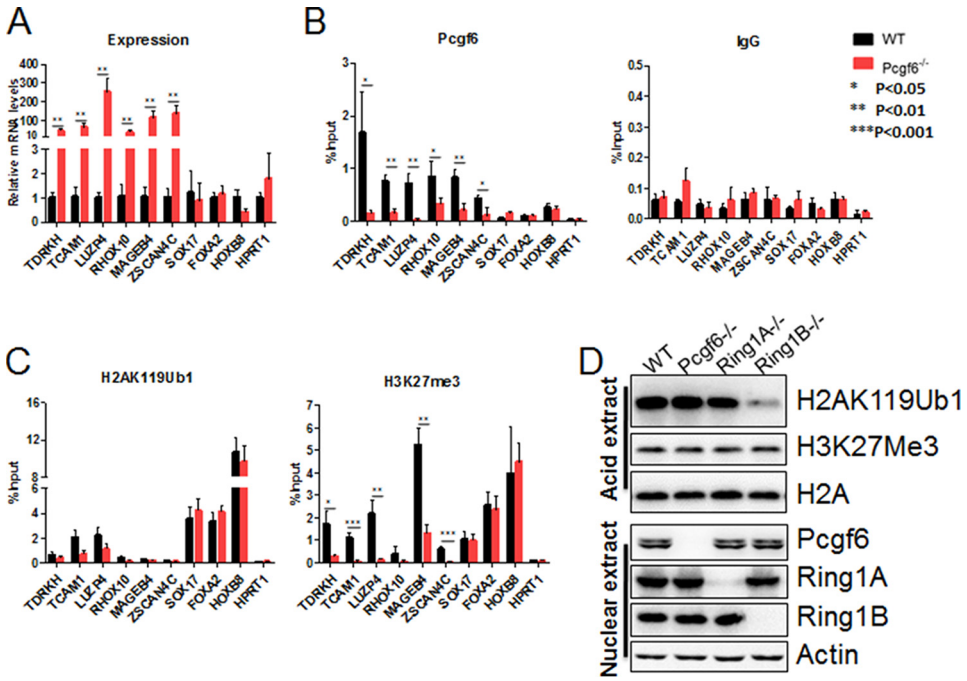

FIGURE 7. **Pcgf6 colocalized with baseline levels of H2AK119ub1 at its target genes.** *A*, expression analysis by RT-qPCR of RNA from ES cells for selected genes. Shown is relative mRNA expression (ratio of measured mRNA/to β-actin mRNA). *B*, ChIP of Pcgf6 followed by quantitative PCR analysis. Purified rabbit IgG was a negative control. *C*, ChIP of H2AK119ub1 and H3K27me3 followed by qPCR analysis of selected gene DNA in ES cells. *A–C*, *bar graphs* represent the mean of three independent biological samples and S.D. Significance: two-tailed Student's *t* test. *D*, Western blot demonstrating changes in the levels of H2AK119ub1, H3K27me3, Pcgf6, Ring1A, and Ring1B in ES cells of indicated genotypes. Histone 2A or β-actin was used as a loading control.

components of PRC1.6, in regulating ES cell self-renewal. Further elucidating of the molecular mechanisms underlying the distinctive transcriptional profile should provide more insight on how PRC1.6 complex orchestrates ES cell self-renewal and differentiation.

Our results clearly show that when Pcgf6 is completely eliminated from ES cells, the cells are highly compromised in their self-renewal ability and undergo skewed differentiation into the endoderm lineage in embryoid bodies (Fig. 3). This is highly reminiscent of the phenotype observed in ES cells deficient in L3mbtl2, another integral component of the PRC1.6 complex (9). However, other studies showed that transient Knockdown of Pcgf6 in ES cells led to lower expression levels of core transcription factor (Oct4, Sox2, and Nanog) (11, 13) and elevated expression of mesodermal lineage markers (12). This discrepancy may indicate that Pcgf6 acts in a dose-dependent manner. Interestingly, Oct-3/4 maintains ES cell characteristics in a dose-dependent manner (31). Transgene-mediated overexpression of a Oct-3/4 <2-fold increase above baseline expression levels in ES cells triggers the differentiation of these cells into primitive endoderm and mesoderm, and reducing the expression of Oct-3/4 induces loss of pluripotency and dedifferentiation to trophectoderm. The expression level of Pcgf6 may affect the fate of ES cells in a similar way. Reduction of Pcgf6 protein to ~20% of endogenous expression levels resulted in elevated expression of mesodermal lineage markers (12), whereas complete disruption of the *Pcgf6* gene led to unscheduled differentiation into the endoderm lineage in embryoid bodies. Therefore, the amount of Pcgf6 must be tightly regulated to maintain stem-cell identity.

The molecular composition of the PRC1.6 complex has been characterized fully by mass spectrometry (8, 9), and several components of this complex have been shown to be essential for ES cell function (9, 29, 30). However, surprisingly little is known about its chromatin-based mechanism for maintaining pluripotency in ES cells. In this study we report the first detailed structure and function of Pcgf6, the core subunit of PRC1.6 complex. We show that Pcgf6 acts as a bridge for the complex assembly interacting with Ring1B, Rybp, and L3mbtl2, and Pcgf6 interacts via the RING motif with Ring1B and Rybp, whereas the C-terminal domain is required for its association with L3mbtl2 (Fig. 6, *A* and *B*). The interaction of Pcgf6 with the chromatin protein L3mbtl2 and the presence of the zinc finger domain (called RING domain in Pcgf6) in both proteins suggest that the Pcgf6 proteins might act as a bridging factor in the PRC1.6 complex for Ring1B and Rybp to act on nucleosomes. To test this hypothesis, we performed chromatin immunoprecipitation assays in ES cells deficient in Pcgf6. As shown in Fig. 8*A*, Ring1B and Rybp occupancy at Pcgf6's selected target genes was significantly reduced in the Pcgf6 null ES cells, supporting the idea that Pcgf6 in the PRC1.6 complex functions to bridge Ring1B and Rybp to chromatin protein L3mbtl2 and/or Max (Fig. 8*A*). This is consistent with our previous observation that L3mbtl2 is required for optimal recruitment of some components (*i.e.* Ring1B, E2F6, G9A, and Hdac1) of PRC1.6 complex to selected germ cell genes (9). Additionally, as shown in Pcgf6, occupancy at target promoters was reduced in L3mbtl2$^{-/-}$ cells. These data clearly show that the Pcgf6-L3mbtl2 interaction is essential for the assembly of PRC1.6 complex and the proper recruitment of the complex to the promoters of target genes *in vivo*.

The noncanonical PRC1 complexes are characterized by the absence of Cbx and Phc subunits and the presence of either Rybp or Yaf2 and, therefore, cannot follow the canonical model

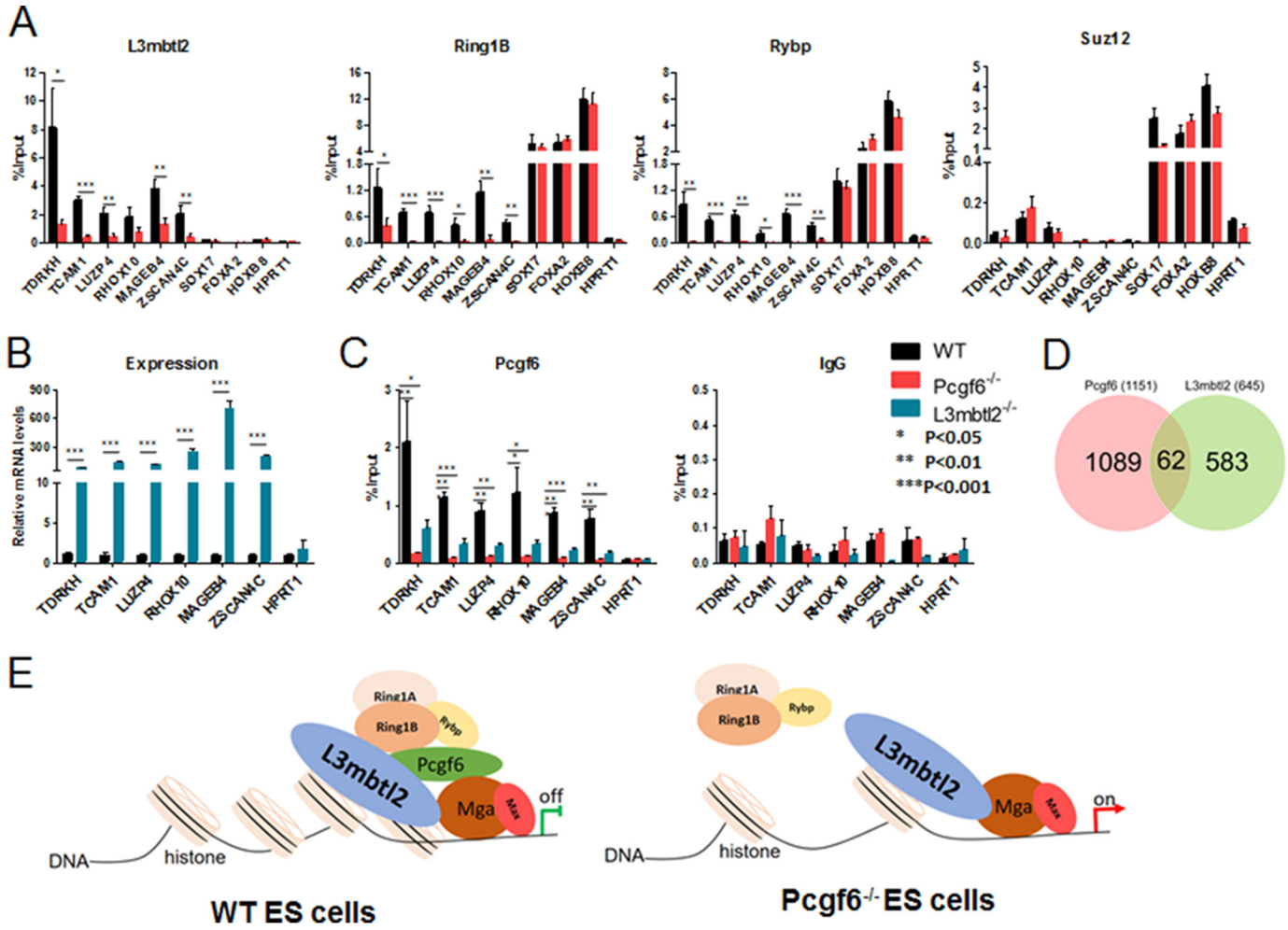

FIGURE 8. **Pcgf6 has a key role in regulating PRC1.6 complex recruitment to its target genes.** *A*, ChIP of L3mbtl2, Ring1B, Rybp, and SUZ12 followed by qPCR analysis of selected gene DNA in ES cells. *B*, expression analysis by RT-qPCR of RNA from ES cells of the indicated genotype for selected genes. *C*, ChIP of Pcgf6 followed by quantitative PCR analysis in ES cells of indicated genotypes. Purified rabbit IgG was a negative control. *A–C*, *bar graphs* represent the mean of three independent biological samples and S.D. Significance: two-tailed Student's *t* test. *D*, Venn diagram illustrating the overlap of L3mbtl2-up-regulated genes with a gene set of Pcgf6-up-regulated target genes. *E*, model showing that the PRC1.6 complex is recruited by Pcgf6-L3mbtl2 interaction and independent of H2AK119ub1 (see "Discussion" for a detailed description).

of dependence of PRC1 on PRC2 (5, 7, 32) for their genomic localization. Our results indicated that although H3K27me3 enrichment at Pcgf6 targets was mildly reduced in the *Pcgf6*$^{-/-}$ ES cells, the baseline levels of occupancy of PRC2 subunits Suz12 at Pcgf6 targets was not altered in Pcgf6 null ES cells compared with wild type (Fig. 7). Additionally, lower amounts of H2AK119ub1 signals were also detected over the promoter regions of Pcgf6 targets and was not affected by loss of Pcgf6 (9). Apparently, our observations suggest an H3K27me3-independent mechanism for the PRC1.6 recruitment on chromatin. This unique characteristic of PRC1.6 gives hints for a possible involvement of the DNA direct binding in the recruitment of this complex (10). Future studies in our laboratory are focused on deciphering the DNA binding ability of components of PRC1.6 (including Mga/Max) responsible for chromatin recruitment, although we previously detect a mild association between genomic L3mblt2 binding sites and E-box motifs which is bound by Mga/Max (9, 33).

Of note, some of PRC1 components exhibit chromatin compaction properties in a histone modification-independent manner: the *Drosophila* Psc (Pcgf paralog) (34), the mouse Ring1B (35), and L3mbtl2 (22). Additionally, it has been shown that the E3 enzymatic activity of Ring1B is dispensable for early mouse development and for global target gene (36) or Hox loci repression (37) in mouse ES cells and in *Drosophila* embryos (38), which raises the question of the precise function of this post-translational modification. We suggest that regulation of chromatin conformation might be central to stable gene silencing by the PRC1.6 complex. Based on our findings, we propose a preliminary model as shown in Fig. 8*E* in Pcgf6 null ES cells; although L3mbtl2 loosely associated with Max/Mga and chromatin, it failed to silence target gene expression due to the disassembly of the PRC1.6 complex. In the presence of Pcgf6, L3mbtl2 interacts with Ring1B and Max/Mga to form a functional multimeric PRC1.6 complex as illustrated in our model to stably repress target genes by compacting chromatin. Future genetic and biochemical experiments should provide evidence for the direct involvement of other components of the PRC1.6 complex, such as Max/Mga, in this process and the precise order in which this complex is recruited to target genes in ES cells.

It is well established that primordial germ cells are initially formed as a cluster (around 40 cells) of Prdm1-positive cells

within the extraembryonic mesoderm near the posterior part of the primitive streak between E6.5 and E7.5 (39). Our microarray analysis reveals that Pcgf6 knock-out in ES cells results in derepression of some germ cell-specific genes (Fig. 4). Thus, Pcgf6 knock-out ES cells may have converted to a germ cell-like state. To test this possibility, we examined the expression of several representative germ cell markers in Pcgf6-deleted ES cells. Real-time PCR shows that expression of early primordial germ cell markers (Prdm1, Dppa3, and Nanos3) (39–42) and meiosis marker (Scp3) (43, 44) in Pcgf6-deleted ES cells is not changed, although expression of some germ cell-specific genes, including Tcam1 and Rhox13, is significantly increased (data not shown), which is consistent with our microarray analysis. Therefore, although Pcgf6 knock-out in ES cells leads to derepression of some germ cell-specific genes, it does not elicit a true germ cell-like state in these cells at least in the experimental conditions in this study. So far, five members of the PRC1.6 complex, Pcgf6, Rybp (45), Max (28, 46), Mga (29), and L3mbtl2 (9), have been reported to be capable of repressing germ cell-related genes in ES cells. A number of studies demonstrated that E2F6, another component of PRC1.6 complex, acted as a repressor of germ cell-related genes in somatic tissues (47–50). Moreover, mutations in l(3)mbt, a *Drosophila* homologue of L3mbtl2, exhibited ectopic expression of germ cell-specific genes in larval brain (51). Therefore, the role of PRC1.6 complex in the repression of germ cell-related gene seems to be at least to some extent cell type-independent or conserved between species. As Pcgf6 is also expressed in adult somatic cells (19), Pcgf6 is likely involved in repression of germ cell-related genes in somatic cells as well. Further studies using mice with a conditional Pcgf6 mutant will provide a unique opportunity to address this aspect.

Experimental Procedures

Mouse ES Cell and MEF Culture—ES cells were cultured with MEFs inactivated with mitomycin-C in DMEM supplemented with 15% fetal calf serum (Gibco), LIF, L-glutamine (Invitrogen), nonessential amino acids (Invitrogen), 0.1 mM β-mercaptoethanol (Sigma), and penicillin/streptomycin (Invitrogen) as described (9). All ES cell lines were maintained at 37 °C in 5% CO_2. MEFs were derived and cultured essentially as described previously (9).

Construction of sgRNAs and Transfection—Genes of interest were assessed for sgRNA specificity and efficiency using MIT's CRISPR Design Tool. The bicistronic expression vector pSp-Cas9 (BB) (pX330; Addgene plasmid ID 42230) was used to express wild type Cas9 under the CBh promoter and the CAG enhancer, and the expression of sgRNA was driven by the strong early U6 promoter (14). The vector was digested with BbsI and then treated with calf intestinal phosphatase to remove terminal phosphates. CACC was added to the 5′ end of the sgRNA-specifying 20-mer and AAAC was added to the 5′ end of the reverse complement of the sgRNA-specifying 20-mer for cloning using the BbsI restriction enzyme. G was added immediately after CACC if the first nucleotide was not G (in these cases C was added at the 3′ end of the reverse complement 20-mer). The adapters served to accommodate ligation into the BbsI-linearized vector. A pair of oligos (Fig. 1*A*, supplemental Figs. 3*A* and 4*A*) for each targeting site was annealed, phosphorylated, and ligated to the linearized vector as follows: guide sequence oligo, guide sequence reverse complement oligo, T4 ligation buffer, and T4 polynucleotide kinase with the following temperature conditions: 37 °C for 2 h, 95 °C for 10 min, and then slowly cooled to room temperature. Linearized vector, 10× buffer and T4 DNA ligase were added to ligation reactions and incubated at 37 °C for 2 h. An aliquot of each reaction was then transformed into a vial of competent cells. Clones containing inserts were sequenced with the U6 forward primer: 5′-ACTATCATATGCTTACCGTAAC-3′. For the deletion of a large segment of genomic DNA we used a pair of sgRNAs against the targeted locus. Two target sites with the pattern N20NGG were selected at the boundary of the target region.

ES cells were seeded onto 6-well plates (Corning) at a density of 5 × 105 cells/well 24 h before transfection. ES Cells were transfected with a total of 2 μg of Cas9 plasmid using Lipofectamine 2000 (Life Technologies) at 80–90% confluency following the manufacturer's recommended protocol. 24 h after transfection ES cells were trypsinized and replated at a low density on feeder layers (DR4 MEFs). Puromycin (4 μg/ml) was added 24 h after replating and taken off after 48 h. After recovering for 7–9 days, individual colonies were picked and genotyped by PCR. Primer sequences are given in supplemental Table 2.

Embryoid Body Formation and Analysis—EB differentiation was performed using the hanging drop method as described (9, 17). Briefly, trypsinized ES cells (10,000 cells/ml) were resuspended in medium without LIF (IMDM, 2 mM L-glutamine, penicillin/streptomycin, nonessential amino acids, 50 μg/ml ascorbic, 200 μg/ml iron-saturated holo-transferrin, 1 mM sodium pyruvate, 450 μM monothioglycerol, and 15% ES cell grade serum). 30 μl (300 cells) were pipetted on Petri dish lids. Hanging drops were cultured for 72 h (37°,5% CO_2). Then EBs were collected from the drops, left in culture in noncoated Petri dishes, and cultured on a rotating shaker (50 rpm, 37 °C, 5% CO_2). Medium was added every 2 days. Total RNA was collected (TRIzol, Invitrogen) at various time points and analyzed by RT-PCR. Primer details are given in supplemental Table 2.

Whole Cell Lysates and Histone Extraction—To obtain whole cell extracts, ES cells were harvested and lysed in radioimmune precipitation assay buffer (50 mM Tris-HCl, pH 8.0, 150 mM NaCl, 1% Triton X-100, 0.5% sodium deoxycholate, 0.1% SDS, 1 mM EDTA, 2 mM Na_3VO_4, 100 mM NaF, 1 mM DTT, 10 mg/ml PMSF, and protease inhibitor mix (Sigma)). Histone extraction and Western blots for histone modifications were performed as described (9, 52). Briefly, histone extraction was performed after two washes with ice-cold PBS and extracted with a Triton extraction buffer (PBS, 0.5% Triton, 2 mm PMSF, 0.02% NaN_3). The lysate was centrifuged, and the pellet was washed twice with Triton extraction buffer and then resuspended in 0.2 N HCl. The nuclei were extracted overnight at 4 °C, and the residue was microcentrifuged for 10 min.

Co-immunoprecipitation and Western Blot Analysis—For coimmunoprecipitation analysis, ES cells were harvested and lysed in radioimmune precipitation assay buffer without SDS.

Cell lysates were clarified by centrifugation, and the supernatant was incubated with antibodies and protein-A/G-Sepharose overnight at 4 °C. Immunoprecipitates were washed 3 times with lysis buffer with 500 mM NaCl, subjected to SDS-PAGE, and probed with the appropriate antibodies as indicated. For controls, either rabbit or mouse IgG antibody was used. All of the antibodies used in this study are listed in supplemental Table 1.

RNA Extraction and Analysis—Cells were first rinsed in PBS and then lysed in TRIzol reagent (Invitrogen). Total RNA was extracted according to the manufacturer's recommendations. RT was carried out with 5 μg of total RNA using Oligo-dT, random hexamers, and Moloney murine leukemia virus reverse transcriptase (Invitrogen). Real-time PCR was performed on a StepOnePlus™ Real-Time PCR Systems with PowerUp™ SYBR Green Master Mix (Applied Biosystems) and analyzed with associated software. Primer sequences are provided in supplemental Table 2.

Microarray Analysis—RNA was isolated from ES cells by disruption in TRIzol reagent (Invitrogen) and was further purified using RNeasy columns (Qiagen) according to the manufacturer's instructions. Total RNA was precipitated with isopropyl alcohol, washed with 70% ethanol, and dissolved in DEPC distilled H_2O. Total RNA (2.5 ug) was labeled with Cy-3 or Cy-5 using an Agilent Low RNA Input Fluorescent Linear Amplification kit. Fluorescently labeled targets were hybridized to SurePrint G3 Mouse Gene Expression 8 × 60K Arrays. Microarray hybridization, scanning (Agilent G2565 CA microarray scanner), and data analysis were performed as described previously (9). Microarray data were deposited at the Gene Expression Omnibus under accession number GSE92476.

ChIP—ChIP was performed essentially as described previously with minor modifications (9). Briefly, formaldehyde was added to a final concentration of 1% for 10 min while gently shaking. Cross-linking was quenched by adding of 125 mm glycine for 5 min. Cells were washed twice with chilled PBS. The pellet was resuspended in lysis buffer (50 mM Tris, pH 8.0, 10 mM EDTA, 1% SDS, protease inhibitors). Chromatin was sheared by sonication (Bioruptor) to around 500-bp fragments. Immunoprecipitation of the chromatin was performed overnight in 1× dilution buffer (16.7 mM Tris, pH 8.0, 1.2 mM EDTA, 0.01% SDS, 1% Triton X-100, 165 mM NaCl, protease inhibitors) with the indicated antibodies. After extensive washes, immunocomplexes were eluted in 1% SDS and 100 mM $NaHCO_3$ at 65 °C. To reverse cross-linking, samples were incubated with 0.3 M NaCl overnight at 65 °C. Samples were purified using Qiagen columns and analyzed by quantitative PCR using gene-specific primer pairs. The fraction of immunoprecipitated material for a specific fragment was calculated by dividing the amount of PCR product obtained from immunoprecipitated DNA by the amount obtained from total DNA (IP/Input). The relative enrichment was calculated as $2^{\Delta Ct}$, where ΔCt = Ct (Input) − Ct (ChIP). Primers utilized for ChIP are listed in supplemental Table 2.

Author Contributions—W. Z. performed the RT-qPCR, ChIP-qPCR, and Pcgf6 structure-function study and analyzed all the experiments. H. T. performed the Western blot analysis. Y. H. genotyped and characterized Pcgf6 knockout ES cells with help from Y. Y. H. T. provided advice on the experimental design and collected and organized the data with the assistance of X. Y. and Q. J. J. Q. designed, performed, analyzed, and supervised the research and wrote the manuscript. The manuscript was critically reviewed and approved by all authors.

Acknowledgments—We thank Drs. Zan Huang and Xiang Gao for providing lentivirus expression vector. We are indebted to Drs. Zhaoyu Lin and Yun Shi for kindly providing reagents and technical advice.

References

1. Simon, J. A., and Kingston, R. E. (2009) Mechanisms of polycomb gene silencing: knowns and unknowns. *Nat. Rev. Mol. Cell Biol.* **10,** 697–708
2. Piunti, A., and Shilatifard, A. (2016) Epigenetic balance of gene expression by Polycomb and COMPASS families. *Science* **352,** aad9780
3. Di Croce, L., and Helin, K. (2013) Transcriptional regulation by Polycomb group proteins. *Nat. Struct. Mol. Biol.* **20,** 1147–1155
4. Richly, H., Aloia, L., and Di Croce, L. (2011) Roles of the Polycomb group proteins in stem cells and cancer. *Cell Death Dis.* **2,** e204
5. Tavares, L., Dimitrova, E., Oxley, D., Webster, J., Poot, R., Demmers, J., Bezstarosti, K., Taylor, S., Ura, H., Koide, H., Wutz, A., Vidal, M., Elderkin, S., and Brockdorff, N. (2012) RYBP-PRC1 complexes mediate H2A ubiquitylation at polycomb target sites independently of PRC2 and H3K27me3. *Cell* **148,** 664–678
6. Morey, L., Pascual, G., Cozzuto, L., Roma, G., Wutz, A., Benitah, S. A., and Di Croce, L. (2012) Nonoverlapping functions of the Polycomb group Cbx family of proteins in embryonic stem cells. *Cell Stem Cell* **10,** 47–62
7. Turner, S. A., and Bracken, A. P. (2013) A "complex" issue: deciphering the role of variant PRC1 in ESCs. *Cell stem cell* **12,** 145–146
8. Gao, Z., Zhang, J., Bonasio, R., Strino, F., Sawai, A., Parisi, F., Kluger, Y., and Reinberg, D. (2012) PCGF homologs, CBX proteins, and RYBP define functionally distinct PRC1 family complexes. *Mol. Cell* **45,** 344–356
9. Qin, J., Whyte, W. A., Anderssen, E., Apostolou, E., Chen, H. H., Akbarian, S., Bronson, R. T., Hochedlinger, K., Ramaswamy, S., Young, R. A., and Hock, H. (2012) The polycomb group protein L3mbtl2 assembles an atypical PRC1-family complex that is essential in pluripotent stem cells and early development. *Cell Stem Cell* **11,** 319–332
10. Ogawa, H., Ishiguro, K., Gaubatz, S., Livingston, D. M., and Nakatani, Y. (2002) A complex with chromatin modifiers that occupies E2F- and Myc-responsive genes in G0 cells. *Science* **296,** 1132–1136
11. Hu, G., Kim, J., Xu, Q., Leng, Y., Orkin, S. H., and Elledge, S. J. (2009) A genome-wide RNAi screen identifies a new transcriptional module required for self-renewal. *Genes Dev.* **23,** 837–848
12. Zdzieblo, D., Li, X., Lin, Q., Zenke, M., Illich, D. J., Becker, M., and Müller, A. M. (2014) Pcgf6, a polycomb group protein, regulates mesodermal lineage differentiation in murine ESCs and functions in iPS reprogramming. *Stem Cells* **32,** 3112–3125
13. Yang, C. S., Chang, K. Y., Dang, J., and Rana, T. M. (2016) Polycomb group protein Pcgf6 acts as a master regulator to maintain embryonic stem cell identity. *Sci. Rep.* **6,** 26899
14. Cong, L., Ran, F. A., Cox, D., Lin, S., Barretto, R., Habib, N., Hsu, P. D., Wu, X., Jiang, W., Marraffini, L. A., and Zhang, F. (2013) Multiplex genome engineering using CRISPR/Cas systems. *Science* **339,** 819–823
15. Mali, P., Yang, L., Esvelt, K. M., Aach, J., Guell, M., DiCarlo, J. E., Norville, J. E., and Church, G. M. (2013) RNA-guided human genome engineering via Cas9. *Science* **339,** 823–826
16. Akasaka, T., van Lohuizen, M., van der Lugt, N., Mizutani-Koseki, Y., Kanno, M., Taniguchi, M., Vidal, M., Alkema, M., Berns, A., and Koseki, H. (2001) Mice doubly deficient for the Polycomb Group genes Mel18 and

Bmi1 reveal synergy and requirement for maintenance but not initiation of Hox gene expression. *Development* **128,** 1587–1597
17. Kurosawa, H. (2007) Methods for inducing embryoid body formation: in vitro differentiation system of embryonic stem cells. *J. Biosci. Bioeng.* **103,** 389–398
18. Wang, P. J., McCarrey, J. R., Yang, F., and Page, D. C. (2001) An abundance of X-linked genes expressed in spermatogonia. *Nat. Genet.* **27,** 422–426
19. Akasaka, T., Takahashi, N., Suzuki, M., Koseki, H., Bodmer, R., and Koga, H. (2002) MBLR, a new RING finger protein resembling mammalian Polycomb gene products, is regulated by cell cycle-dependent phosphorylation. *Genes Cells* **7,** 835–850
20. Endoh, M., Endo, T. A., Endoh, T., Fujimura, Y., Ohara, O., Toyoda, T., Otte, A. P., Okano, M., Brockdorff, N., Vidal, M., and Koseki, H. (2008) Polycomb group proteins Ring1A/B are functionally linked to the core transcriptional regulatory circuitry to maintain ES cell identity. *Development* **135,** 1513–1524
21. Wu, H., Chen, X., Xiong, J., Li, Y., Li, H., Ding, X., Liu, S., Chen, S., Gao, S., and Zhu, B. (2011) Histone methyltransferase G9a contributes to H3K27 methylation *in vivo*. *Cell Res.* **21,** 365–367
22. Trojer, P., Cao, A. R., Gao, Z., Li, Y., Zhang, J., Xu, X., Li, G., Losson, R., Erdjument-Bromage, H., Tempst, P., Farnham, P. J., and Reinberg, D. (2011) L3MBTL2 protein acts in concert with PcG protein-mediated monoubiquitination of H2A to establish a repressive chromatin structure. *Mol. Cell* **42,** 438–450
23. Sánchez, C., Sánchez, I., Demmers, J. A., Rodriguez, P., Strouboulis, J., and Vidal, M. (2007) Proteomics analysis of Ring1B/Rnf2 interactors identifies a novel complex with the Fbxl10/Jhdm1B histone demethylase and the Bcl6 interacting corepressor. *Mol. Cell. Proteomics* **6,** 820–834
24. Luis, N. M., Morey, L., Di Croce, L., and Benitah, S. A. (2012) Polycomb in stem cells: PRC1 branches out. *Cell Stem Cell* **11,** 16–21
25. Chamberlain, S. J., Yee, D., and Magnuson, T. (2008) Polycomb repressive complex 2 is dispensable for maintenance of embryonic stem cell pluripotency. *Stem Cells* **26,** 1496–1505
26. Pasini, D., Bracken, A. P., Jensen, M. R., Lazzerini Denchi, E., and Helin, K. (2004) Suz12 is essential for mouse development and for EZH2 histone methyltransferase activity. *EMBO J.* **23,** 4061–4071
27. Leeb, M., and Wutz, A. (2007) Ring1B is crucial for the regulation of developmental control genes and PRC1 proteins but not X inactivation in embryonic cells. *J. Cell Biol.* **178,** 219–229
28. Maeda, I., Okamura, D., Tokitake, Y., Ikeda, M., Kawaguchi, H., Mise, N., Abe, K., Noce, T., Okuda, A., and Matsui, Y. (2013) Max is a repressor of germ cell-related gene expression in mouse embryonic stem cells. *Nat. Commun.* **4,** 1754
29. Washkowitz, A. J., Schall, C., Zhang, K., Wurst, W., Floss, T., Mager, J., and Papaioannou, V. E. (2015) Mga is essential for the survival of pluripotent cells during peri-implantation development. *Development* **142,** 31–40
30. Hishida, T., Nozaki, Y., Nakachi, Y., Mizuno, Y., Okazaki, Y., Ema, M., Takahashi, S., Nishimoto, M., and Okuda, A. (2011) Indefinite self-renewal of ESCs through Myc/Max transcriptional complex-independent mechanisms. *Cell Stem Cell* **9,** 37–49
31. Niwa, H., Miyazaki, J., and Smith, A. G. (2000) Quantitative expression of Oct-3/4 defines differentiation, dedifferentiation or self-renewal of ES cells. *Nat. Genet.* **24,** 372–376
32. He, J., Shen, L., Wan, M., Taranova, O., Wu, H., and Zhang, Y. (2013) Kdm2b maintains murine embryonic stem cell status by recruiting PRC1 complex to CpG islands of developmental genes. *Nat. Cell Biol.* **15,** 373–384
33. Conacci-Sorrell, M., McFerrin, L., and Eisenman, R. N. (2014) An overview of MYC and its interactome. *Cold Spring Harb. Perspect. Med.* **4,** a014357
34. Francis, N. J., Kingston, R. E., and Woodcock, C. L. (2004) Chromatin compaction by a polycomb group protein complex. *Science* **306,** 1574–1577
35. Eskeland, R., Leeb, M., Grimes, G. R., Kress, C., Boyle, S., Sproul, D., Gilbert, N., Fan, Y., Skoultchi, A. I., Wutz, A., and Bickmore, W. A. (2010) Ring1B compacts chromatin structure and represses gene expression independent of histone ubiquitination. *Mol. Cell* **38,** 452–464
36. Illingworth, R. S., Moffat, M., Mann, A. R., Read, D., Hunter, C. J., Pradeepa, M. M., Adams, I. R., and Bickmore, W. A. (2015) The E3 ubiquitin ligase activity of RING1B is not essential for early mouse development. *Genes Dev.* **29,** 1897–1902
37. Endoh, M., Endo, T. A., Endoh, T., Isono, K., Sharif, J., Ohara, O., Toyoda, T., Ito, T., Eskeland, R., Bickmore, W. A., Vidal, M., Bernstein, B. E., and Koseki, H. (2012) Histone H2A mono-ubiquitination is a crucial step to mediate PRC1-dependent repression of developmental genes to maintain ES cell identity. *PLoS genetics* **8,** e1002774
38. Pengelly, A. R., Kalb, R., Finkl, K., and Müller, J. (2015) Transcriptional repression by PRC1 in the absence of H2A monoubiquitylation. *Genes Dev.* **29,** 1487–1492
39. Saitou, M., Barton, S. C., and Surani, M. A. (2002) A molecular programme for the specification of germ cell fate in mice. *Nature* **418,** 293–300
40. Ohinata, Y., Payer, B., O'Carroll, D., Ancelin, K., Ono, Y., Sano, M., Barton, S. C., Obukhanych, T., Nussenzweig, M., Tarakhovsky, A., Saitou, M., and Surani, M. A. (2005) Blimp1 is a critical determinant of the germ cell lineage in mice. *Nature* **436,** 207–213
41. Tsuda, M., Sasaoka, Y., Kiso, M., Abe, K., Haraguchi, S., Kobayashi, S., and Saga, Y. (2003) Conserved role of nanos proteins in germ cell development. *Science* **301,** 1239–1241
42. Suzuki, A., Tsuda, M., and Saga, Y. (2007) Functional redundancy among Nanos proteins and a distinct role of Nanos2 during male germ cell development. *Development* **134,** 77–83
43. Yuan, L., Liu, J. G., Zhao, J., Brundell, E., Daneholt, B., and Höög, C. (2000) The murine SCP3 gene is required for synaptonemal complex assembly, chromosome synapsis, and male fertility. *Mol. Cell* **5,** 73–83
44. Yuan, L., Liu, J. G., Hoja, M. R., Wilbertz, J., Nordqvist, K., and Höög, C. (2002) Female germ cell aneuploidy and embryo death in mice lacking the meiosis-specific protein SCP3. *Science* **296,** 1115–1118
45. Hisada, K., Sánchez, C., Endo, T. A., Endoh, M., Román-Trufero, M., Sharif, J., Koseki, H., and Vidal, M. (2012) RYBP represses endogenous retroviruses and preimplantation- and germ line-specific genes in mouse embryonic stem cells. *Mol. Cell. Biol.* **32,** 1139–1149
46. Suzuki, A., Hirasaki, M., Hishida, T., Wu, J., Okamura, D., Ueda, A., Nishimoto, M., Nakachi, Y., Mizuno, Y., Okazaki, Y., Matsui, Y., Izpisua Belmonte, J. C., and Okuda, A. (2016) Loss of MAX results in meiotic entry in mouse embryonic and germline stem cells. *Nat. Commun.* **7,** 11056
47. Pohlers, M., Truss, M., Frede, U., Scholz, A., Strehle, M., Kuban, R. J., Hoffmann, B., Morkel, M., Birchmeier, C., and Hagemeier, C. (2005) A role for E2F6 in the restriction of male-germ-cell-specific gene expression. *Curr. Biol.* **15,** 1051–1057
48. Kehoe, S. M., Oka, M., Hankowski, K. E., Reichert, N., Garcia, S., McCarrey, J. R., Gaubatz, S., and Terada, N. (2008) A conserved E2F6-binding element in murine meiosis-specific gene promoters. *Biol. Reprod.* **79,** 921–930
49. Velasco, G., Hubé, F., Rollin, J., Neuillet, D., Philippe, C., Bouzinba-Segard, H., Galvani, A., Viegas-Péquignot, E., and Francastel, C. (2010) Dnmt3b recruitment through E2F6 transcriptional repressor mediates germ-line gene silencing in murine somatic tissues. *Proc. Natl. Acad. Sci. U.S.A.* **107,** 9281–9286
50. Storre, J., Schäfer, A., Reichert, N., Barbero, J. L., Hauser, S., Eilers, M., and Gaubatz, S. (2005) Silencing of the meiotic genes SMC1β and STAG3 in somatic cells by E2F6. *J. Biol. Chem.* **280,** 41380–41386
51. Janic, A., Mendizabal, L., Llamazares, S., Rossell, D., and Gonzalez, C. (2010) Ectopic expression of germline genes drives malignant brain tumor growth in *Drosophila*. *Science* **330,** 1824–1827
52. Qin, J., Van Buren, D., Huang, H. S., Zhong, L., Mostoslavsky, R., Akbarian, S., and Hock, H. (2010) Chromatin protein L3MBTL1 is dispensable for development and tumor suppression in mice. *J. Biol. Chem.* **285,** 27767–27775